

Sensor phenomena

Microwave Dielectric Sensing in Hyperbolically Dispersive MediaOmar F. Siddiqui¹  and Ashraf S. Mohra²¹*College of Engineering, Taibah University, Madinah 41477, Saudi Arabia*²*Electrical Engineering Department, Faculty of Engineering, Benha University, Benha 13511, Egypt*

Manuscript received September 19, 2017; revised October 4, 2017; accepted October 19, 2017. Date of publication November 2, 2017; date of current version November 15, 2017.

Abstract— We propose microwave dielectric sensing by exploiting the highly sensitive frequency response of hyperbolically dispersive media. Through dispersion analysis, we show that the hyperbolic media are both spatially and spectrally sensitive to very slight changes in the constitutive dielectric material. We practically demonstrate the concept of microwave sensing in microstrip-based metallic grid structure cells fabricated on a grounded dielectric substrate. High dielectric sensitivities are shown when dielectric samples are placed in the path of the resonance cones, which are the characteristic high-field regions in hyperbolic medium under resonance. We demonstrate the resonant frequency shifts for the relative permittivities in the range of 1–3.5.

Index Terms—Sensor phenomena, resonant plasma, resonance sensor, microwave sensors, dielectric constant, hyperbolic dispersion.

I. INTRODUCTION

The hyperbolic dispersion and the associated resonance-cones formation are perhaps the most interesting physical effects that occur in anisotropic plasmas [1], [2]. The hyperbolic dispersion surfaces are formed when plasma is under resonance and two of the diagonal entries of the permittivity matrix become oppositely signed. Consequently, the electrical fields travel in conical shapes of spatial resonance patterns known as the “resonance-cones.” Under the lossless conditions, the refractive index and the power density in the resonance-cone direction become infinite. This particular mathematical singularity attracted the attention of many mathematicians and physicists during the 1970’s towards the problem of plasma wave propagation [2]. The trend of artificial media synthesis (metamaterials) in the past decade stirred a renewed interest in the plasma wave propagation [3], [4]. The unique plasma-wave propagation stems from its specific dispersion profile characterized by “open” phase (k) surfaces with elongated asymptotes, which allow the large wavevectors (that otherwise become evanescent) to propagate within the hyperbolic media [5]. Furthermore, the group velocity vectors that emanate from the asymptotic k -space point in the same direction forming high intensity frequency-dependent narrow beams (the resonance cones) [4], [6]. Microwave and optical metamaterials that emulate the plasma-like dispersion have been proposed for interesting applications [7] such as spatial filtering [8], [9], near-field imaging [10], and biosensing [11], [12].

The fact that the spatial and spectral properties of the resonant-cone fields strongly depend on the surrounding environment makes the hyperbolic media excellent candidates for dielectric sensing. Recently, highly sensitive biosensor has been fabricated by alternatively depositing thin gold and aluminum dioxide films to form a layered hyperbolic structure that operates in the visible light near infrared spectrum [11]. The changes in the biosamples were detected by injecting them in

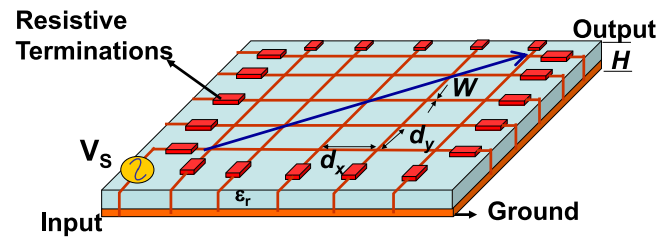


Fig. 1. Hyperbolically dispersive metallic grid with the arrow indicating the direction of the resonance-cone.

the structure and sensing the resonance shifts. In another research work, a hyperbolic metamaterial was numerically configured using gold nanorods and the refractive index of the host material was estimated by determining the angular variation of the reflected optical beam [12].

In this article, we exploit the hyperbolic dispersion for dielectric sensing at *microwave* frequencies. A much simpler hyperbolic structure is considered [8], which consists of a metallic grid printed on a grounded dielectric substrate with a relative permittivity of ϵ_r (see Fig. 1). The sensing principle is theoretically demonstrated via dispersion analysis and practically implemented in a fabricated device. The proposed sensing scheme falls in the category of the narrow-band resonant sensors traditionally applied to characterize dielectric samples in a spectrum [13].

II. DISPERSION ANALYSIS AND SENSING MECHANISM

Referring to Fig. 1, note that the anisotropy that leads to the hyperbolic dispersion is obtained by designing the rectangular unit cells with unequal arms d_x and d_y such that the combined intrinsic phase shift is equal to 2π at the resonant frequency [6], [8]. Mathematically this resonance condition is given by

$$\beta d_x + \beta d_y = 2\pi. \quad (1)$$

Corresponding author: Omar F. Siddiqui (e-mail: omarsiddiqui2@gmail.com).

Associate Editor: G. Langfelder.

Digital Object Identifier 10.1109/LSENS.2017.2768320

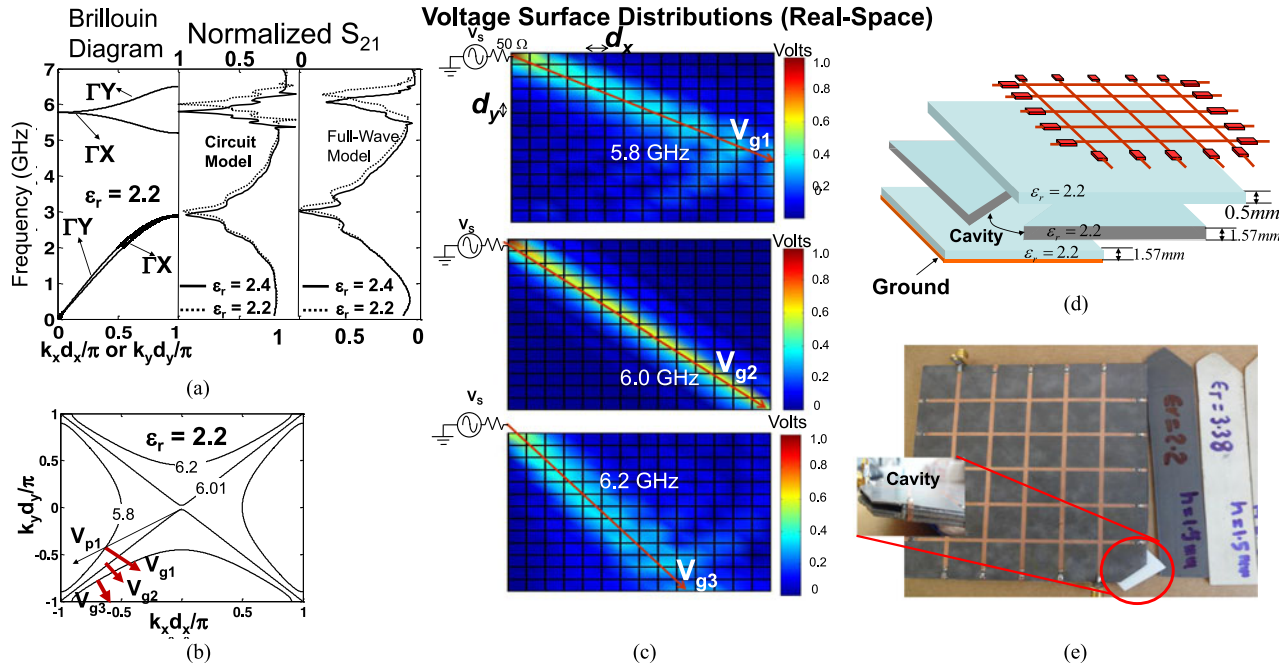


Fig. 2. (a) Band structure of the infinitely extended hyperbolic grid accompanied with two S_{21} simulations of the truncated version showing the spectral sensing. The circuit analysis and the full-wave simulations are performed using the Agilents ADS and Momentum packages. (b) Iso-frequency dispersion surfaces showing the energy propagation in k-space. (c) Energy propagation in the real-space derived from the k-space showing the propagation of resonance cones in different v_g directions corresponding to the three frequencies (spatial sensing). (d) Hyperbolic sensor designed using a three-layered dielectric structure with a cavity. (e) Photograph of the fabricated device. The inset shows the cavity for the sample.

Applying the Bloch-Floquet condition, the following dispersion equation can be obtained [6], [14]:

$$\sin(\beta d_x) \cos(k_y d_y) + \sin(\beta d_y) \cos(k_x d_x) = \sin(\beta d_x + \beta d_y) \quad (2)$$

where k_x and k_y are the Bloch propagation constants. At an angular frequency of ω , the intrinsic microstrip propagation constant β [15] is given by

$$\beta = \frac{\omega}{c} \sqrt{\frac{\epsilon_r + 1}{2} + \frac{\epsilon_r - 1}{2\sqrt{1 + 12H/W}}}, \quad (3)$$

H represents the thickness of the substrate, and W is the width of the microstrip traces, as shown in Fig. 1. The resulting band structure (Brillouin diagram) is depicted in Fig. 2(a). To identify the resonance points, the Brillouin diagram is also accompanied by a transmission coefficient (S_{21}) simulation of the terminated hyperbolic grid of Fig. 1. The lowest of the two resonance modes at 3 GHz is the wideband Bragg mode which is common to all the periodic structures. Our mode of interest is the hyperbolic mode which is identified by a narrowband S_{21} peak at 6 GHz. This resonance is characterized by the intersection of a forward wave in Γ_Y direction and a backward wave in Γ_X direction. More interestingly, when the lossless resonance condition (1) is substituted in the dispersion (2), the resulting k-surface becomes a pair of intersecting line, i.e., $k_y d_y = \pm k_x d_x$.

The unique ability of the hyperbolic structures to be exploited as both spatial (angular) and spectral sensors can be observed by considering the Brillouin diagram and the associated the k-surfaces depicted in Fig. 2. Just above or below the resonance of 6 GHz, the k-surfaces take hyperbolic shapes with an orthogonal relationship between the phase velocity (v_p) and the group velocity (v_g) vectors. The resonance-cone formation and the associated enhanced electric field propagation

result from the emergence of the co-directional v_g -vectors from the hyperbolic asymptotes leading to the peak in the S_{21} plot. The spatial sensing aspect can be explained by observing the change in the asymptotic slope of the hyperbolic k-surface with the change in frequency or the substrate's intrinsic permittivity. Consequently, as indicated in the real space plot of Fig. 2(c), obtained by the Forward Transmission Matrix (FTM) method [20], the v_g -vectors and the resulting resonance-cones travel in different directions for the three indicated frequencies. The resonance-cone direction, in this case, depend on the slope of the asymptotes and the dielectric constant of the host substrate.

The spectral sensing mechanism can be highlighted by observing the fact that with the increase in the dielectric constant of the host substrate ϵ_r , the intrinsic propagation constant (3) also increases, thereby forcing the resonance condition (1) to be satisfied at a lower frequency. To show the enhanced sensitivity, the host dielectric constant was slightly changed from 2.2 to 2.4. As indicated in the dotted S_{21} graph of Fig. 2, the hyperbolic structure is able to resolve this change by shifting the resonance from 6 GHz to 5.8 GHz. The overall sensitivity achieved by this 4x4 cell hyperbolic structure is about 3.18 GHz per refractive index unit (RIU) which compares well with some of the contemporary sensing methods given in Table 1. Here, refractive index for non-magnetic materials is calculated by the relation $n = \sqrt{\epsilon_r}$. Note that in some of the current sensor topologies, increased sensitivities and high experimental Q-factors reaching 2000 are obtained by much complex periodic structures such as [19] where host substrate had to be modified by placing dielectric resonator arrays.

To assess the performance of the sensing device, a figure of merit (FOM) is usually specified. In this case, we define a FOM that is directly proportional to its sensitivity and inversely proportional to the resonance's full width at half maximum (FWHM), and therefore, it

Table 1. Comparison of Contemporary Sensors.

Sensor Type	Sensitivity (S) in GHz/RIU
	$S = \frac{\text{Resonance-shift}}{\sqrt{\epsilon_r} - \sqrt{\epsilon_r 1}}$
Photonic-Crystal Phase Sensor [16]	0.47
Anomalous Phase Sensor [17]	1.1
Epsilon-near-zero Sensor [18]	2.45
Proposed Hyperbolic Sensor	3.180
Fano-resonance Sensor [19]	4.02

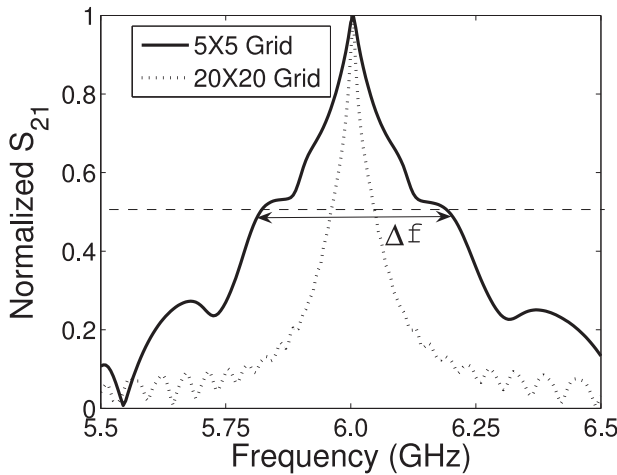


Fig. 3. Comparison of the transmission responses of a five-cell and 20-cell hyperbolic grid.

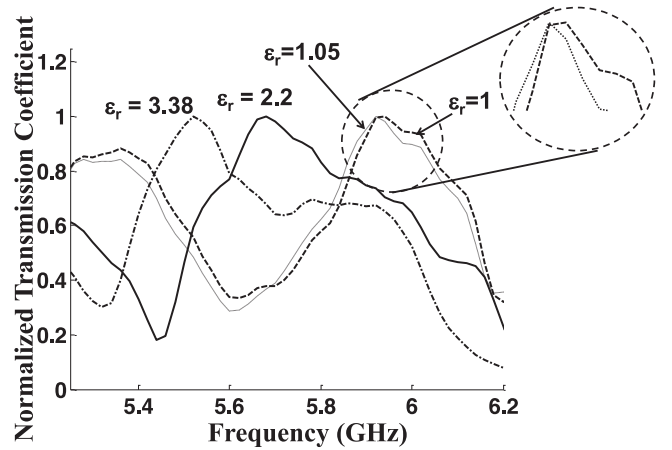
indicates the resonance's sharpness and the sensor's selectivity [11]:

$$FOM = \frac{\Delta f_r}{\Delta n \Delta f} \quad (4)$$

where Δf_r is the resonance shift for a change of Δn in the refractive index and Δf is the resonance's FWHM. Since the FOM is inversely proportional to FWHM (Δf), a sensor with sharp resonant response (high-Q) can resolve close permittivities more effectively. We observe by applying simple circuit rules to Fig. 1 that the quality factor of the hyperbolic grid (and, consequently, the FOM) can be further improved by simply incorporating more unit cells. The extended circuit in this case behaves as several cascaded filters connected in series. For comparison, the transmission responses of five-cell and 20-cell hyperbolic grids are calculated by the FTM method [20] and plotted in Fig. 3. The numerical analysis of the transmission response show an increase of Q-factor from 50 to 200 when the number of unit cells are increased from 5 to 20. The increased device size in this case can be reduced by printing the metallic grids on high dielectric substrates. This can be understood by noting the increase in the intrinsic propagation constant β in (3), when the dielectric constant ϵ_r is increased. Consequently, the dispersion equation (1) is satisfied for smaller unit cell lengths d_x and d_y .

III. A PRACTICAL HYPERBOLIC SENSING SCHEME

An experimental set up to verify the spectral sensing principle in the hyperbolic media was devised by constructing a three layer dielectric structure using Rogers 5880 material with a cavity in the central layer to place the sample, as depicted in Fig. 2(d) and (e). Four samples of dielectric materials i.e., air, foam, Rogers 5880, and Rogers 4003

Fig. 4. Measured S_{21} coefficients for different dielectric samples placed in the hyperbolic sensor's cavity

materials having respective dielectric constants of 1, 1.05, 2.2, and 3.38 were cut into appropriate sizes to be inserted into the cavity. The S_{21} magnitudes (see Fig. 4) were measured with the help of Rohde and Schwarz, ZVA67 Vector Network Analyzer and the peak frequencies were detected for permittivity characterization. With the Rogers 5880 sample, the peak in the S_{21} gave the sensor's characteristic frequency. A shift from this frequency (5.68 GHz) indicate the dielectric permittivity shift. Hence, if the cavity was filled with higher permittivity samples, redshifts in the resonance would be detected, as depicted in Fig. 4 for Rogers 4003. On the other hand, with lower than 2.2 relative permittivities such as air and foam samples, resonance blueshifts, i.e., 5.94 and 5.92 GHz were obtained. Note the slight resonance shift between air and foam samples, the sensor was able to resolve, showing the enhanced sensitivity of the proposed scheme. While the presented experiment demonstrates the concept of dielectric sensing using hyperbolic materials, a practical sensor prototype can be devised by calibrating these resonance shifts with standard permittivity materials. The high-Q hyperbolic sensors can be the potentially alternatives to the expensive optical sensors that are currently used in applications where resolution of very close permittivities is desired such as sensing gaseous media [21].

IV. CONCLUSION

We propose highly sensitive dielectric detection based on the hyperbolically dispersive modes. The enhanced sensitivity is obtained by placing the samples in the path of the resonance-cones which are intense electromagnetic fields that propagate in hyperbolic media under resonance. We show experimentally that a hyperbolic structure based on a simple microstrip transmission-line grid is able to detect reasonable frequency shifts for several dielectric samples. We anticipate that with the offered sensitivity, the proposed sensing method can be used to characterize close-valued permittivities.

REFERENCES

- [1] R. Fisher and R. Gould, "Resonance cones in the field pattern of a short antenna in an anisotropic plasma," *Phys. Rev. Lett.*, vol. 22, pp. 1093–1095, May 1969.
- [2] R. Fisher and R. Gould, "Resonance cones in the field pattern of a radio frequency probe in a warm anisotropic plasma," *Phys. Fluids*, vol. 15, pp. 857–867, Apr. 1971.

- [3] G. V. Eleftheriades and K. G. Balmain, *Negative-Refraction Metamaterials: Fundamental Principles and Applications*. New York, NY, USA: Wiley, 2005.
- [4] K. G. Balmain, A. Luttgen, and P. C. Kremer, "Resonance cone formation, reflection, refraction, and focusing in a planar anisotropic metamaterial," *IEEE Antennas Wireless Propag. Lett.*, vol. 1, no. 1, pp. 146–149, 2002.
- [5] D. Schurig and D. Smith, "Sub-diffraction imaging with compensating bilayers," *New J. Phys.*, vol. 7, no. 1, pp. 162–176, 2005.
- [6] G. V. Eleftheriades and O. F. Siddiqui, "Negative refraction and focusing in hyperbolic transmission-line periodic grids," *IEEE Trans. Microw. Theory Techn.*, vol. 53, no. 1, pp. 396–403, Jan. 2005.
- [7] P. Shekhar, J. Atkinson, and Z. Jacob, "Hyperbolic metamaterials: Fundamentals and applications," *Nano Convergence*, vol. 1, no. 1, pp. 1–17, 2014.
- [8] O. F. Siddiqui and G. V. Eleftheriades, "Resonant modes in continuous metallic grids over ground and related spatial-filtering applications," *J. Appl. Phys.*, vol. 99, no. 8, 2006, Art. no. 083102. [Online]. Available: <http://scitation.aip.org/content/aip/journal/jap/99/8/10.1063/1.2189929>
- [9] X. Zhou, X. Yin, T. Zhang, L. Chen, and X. Li, "Ultrabroad terahertz bandpass filter by hyperbolic metamaterial waveguide," *Opt. Exp.*, vol. 23, no. 9, pp. 11 657–11 664, May 2015.
- [10] A. Salandrino and N. Engheta, "Far-field subdiffraction optical microscopy using metamaterial crystals: Theory and simulations," *Phys. Rev. B*, vol. 74, no. 7, 2006, Art. no. 075103.
- [11] K. V. Sreekanth *et al.*, "Extreme sensitivity biosensing platform based on hyperbolic metamaterials," *Nature Mater.*, vol. 15, no. 6, pp. 621–627, 2016.
- [12] N. Vasilantonakis, G. Wurtz, V. Podolskiy, and A. Zayats, "Refractive index sensing with hyperbolic metamaterials: Strategies for biosensing and nonlinearity enhancement," *Opt. Exp.*, vol. 23, no. 11, pp. 14 329–14 343, 2015.
- [13] L. Chen, C. Ong, C. Neo, V. Varadan, and V. Varadan, *Microwave Electronics: Measurement and Materials Characterization*. Chichester, U.K.: Wiley, 2004.
- [14] A. Grbic and G. V. Eleftheriades, "Periodic analysis of a 2-d negative refractive index transmission line structure," *IEEE Trans. Antennas Propag.*, vol. 51, no. 10, pp. 2604–2611, Oct. 2003.
- [15] D. M. Pozar, *Microwave Engineering*. New York, NY, USA: Wiley, 2005, pp. 143–145.
- [16] Á. Andueza, J. Pérez-Conde, and J. Sevilla, "Differential refractive index sensor based on photonic molecules and defect cavities," *Opt. Exp.*, vol. 24, no. 16, pp. 18 807–18 816, Aug. 2016. [Online]. Available: <http://www.opticsexpress.org/abstract.cfm?URL=oe-24-16-18807>
- [17] R. Ramzan, O. Siddiqui, W. Arshad, and O. Ramahi, "A novel material parameter extraction method based on anomalous dispersion," *IEEE Trans. Microw. Theory Techn.*, vol. 64, no. 11, pp. 3787–3796, Nov. 2016.
- [18] A. Alù and N. Engheta, "Dielectric sensing in -near-zero narrow waveguide channels," *Phys. Rev. B*, vol. 78, Jul. 2008, Art. no. 045102. [Online]. Available: <http://link.aps.org/doi/10.1103/PhysRevB.78.045102>
- [19] E. Semouchkina, R. Duan, G. Semouchkin, and R. Pandey, "Sensing based on fano-type resonance response of all-dielectric metamaterials," *Sensors*, vol. 15, no. 4, pp. 9344–9359, 2015.
- [20] O. Siddiqui, "The forward transmission matrix method for s-parameter analysis of microwave circuits and their metamaterial counterparts," *Progress Electromagn. Res. B*, vol. 66, pp. 123–141, 2016.
- [21] H. Clevenson, P. Desjardins, X. Gan, and D. Englund, "High sensitivity gas sensor based on high-Q suspended polymer photonic crystal nanocavity," *Appl. Phys. Lett.*, vol. 104, no. 24, 2014, Art. no. 241108.